International Journal of Concrete Structures and Materials
Vol.11, No.2, pp.275–284, June 2017
DOI 10.1007/s40069-017-0188-5
ISSN 1976-0485 / eISSN 2234-1315

An Estimate of the Yield Displacement of Coupled Walls for Seismic Design

Enrique Hernández-Montes[1),*], and Mark Aschheim[2)]

(Received August 26, 2016, Accepted January 31, 2017, Published online May 29, 2017)

Abstract: A formula to estimate the yield displacement observed in the pushover analysis of coupled wall lateral force-resisting systems is presented. The estimate is based on the results of an analytical study of coupled walls ranging from 8 to 20 stories in height, with varied amounts of reinforcement in the reinforced concrete coupling beams and walls, subjected to first-mode pushover analysis. An example illustrates the application of these estimates to the performance-based seismic design of coupled walls.

Keywords: coupled walls, shear walls, earthquake engineering.

1. Introduction

Some displacement-based methods for seismic design (Aschheim and Black 2000; Aschheim 2000; Paulay 2002) use an estimate of the yield displacement as a basis for establishing values of critical design parameters such as base shear strength. In contrast to the lateral stiffness or fundamental period of vibration, whose values are unknown at the beginning of the design process and vary with the lateral strength provided to the structure, the yield displacement is a kinematic quantity and varies little with changes in lateral strength. Figure 1 illustrates the base shear resistance developed by two building models under a constant (increasing) lateral force profile, as a function of the displacement of the roof. The only difference between the two models is the amount of reinforcement. While the strength and stiffness differ, the yield displacement is nearly invariant, and can be estimated based on kinematic relationships associated with strains, member dimensions, and structural geometry, for the usual distributions of mass and stiffness in a structural system (Aschheim and Black 2000). In contrast, conventional seismic design approaches are based on the fundamental period of vibration. The period is a function of the stiffness of the structure (assuming the mass of the building is kept constant) which in turn depends on the amount of reinforcing steel and concrete in the member cross sections and hence changes as member strengths are adjusted to achieve the intended seismic performance goals. This dependence of period on lateral strength, if represented accurately in the model, causes period-based seismic design approaches to require a larger number of iterations than are needed with approaches that are based on the yield displacement. If the variation of stiffness with strength is not represented in the model, the analytical results are likely to be of poor fidelity and may lead to an imprecise characterization of the suitability of the design relative to the seismic performance goals.

Because changes in lateral strength are achieved by changing the amount of material used, rather than the inherent strengths of the steel and concrete materials, the changes in lateral strength are associated with changes in lateral stiffness. The yield displacement observed in a nonlinear static (pushover) analysis is nearly invariant with changes in lateral strength. This is easily explained for individual structural elements (Priestley et al. 1995; Hernández-Montes and Aschheim 2003), and is also observed in a more generalized way for entire buildings (Paulay 2002; Tjhin et al. 2007).

Recognition of the stability of the yield displacement has led to work in recent years to provide formulas to estimate the yield displacement and yield curvature of various structural elements (e.g., columns and beams of various cross-sectional shapes) as well as structural systems comprised of walls or frames and dual systems. As an illustration, relatively current approximations for the effective yield curvature of reinforced concrete (RC) members and steel members are (Priestley et al. 2007) given in Table 1.

Priestley et al. (2007) provide a method to estimate the yield displacement of coupled walls which relies on the degree of coupling of the beams, β_{CB}, quantified as:

$$\beta_{CB} = \frac{M_{CB,b}}{M_{OTM}} \tag{1}$$

where $M_{CB,b}$ is the base moment resistance associated with a couple resulting from the shears carried by the coupling beams and M_{OTM} is the overturning moment at the base

[1)]Universidad de Granada, Granada, Spain.
*Corresponding Author; E-mail: emontes@ugr.es
[2)]Santa Clara University, Santa Clara, USA.

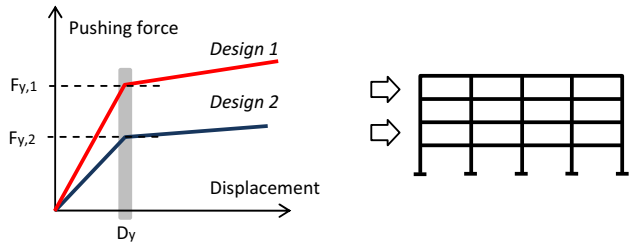

Fig. 1 Results of pushover analysis, for models that differ only in component reinforcement quantity.

induced by the applied lateral loads. The yield displacement of the wall is then estimated by considering curvatures over the height of a wall, recognizing that the influence of coupling beam resistance on the bending moments within the walls. The degree of coupling beam, β_{CB}, affects the location of zero moment within the wall, and is determined from empirical studies.

2. Behavioral Assumptions for Coupled Walls

Coupled walls can be considered to be an extension of the strong-column weak-beam philosophy of seismic design, applied to shear walls. This philosophy seeks to ensure that primary elements critical to structural integrity maintain gravity load resistance throughout the seismic action, while yielding develops within the beams. Yielding at the base of the columns or walls is accepted as an unavoidable part of the mechanism that develops during inelastic response, although yielding of the beams is the preferred way to confer ductility to the lateral force-resisting system.

The lateral response of coupled walls is complex because the coupling beams generally yield first, in a sequence that emerges as the lateral displacements increase, and prior to flexural yielding at the base of each wall pier. Coupling beams within a coupled wall system can be chosen to be identical, having the same dimensions and reinforcement over the height of the coupled wall system. The amount of shear resisted by the coupling beams over the height of the system at one instant during the linear elastic portion of response in a first-mode pushover analysis of a 12-story coupled wall is shown in Fig. 2. The results obtained are similar to those described in Naeim (2001). The deformed shape was obtained using a commercial software package SeismoStruct (2016), in which inelastic fiber elements were used to represent the flexural and axial response of the wall and coupling beams, while linear elastic resistance to shear was modeled. One may observe the wall profile is nearly linear above the location of peak coupling beam shear.

An estimate of the yield displacement observed in a first-mode nonlinear static (pushover) analysis is useful for seismic design. In such an analysis, lateral forces are applied over the height of the building in proportion to the amplitude of the first mode, $\phi_{1,i}$ and mass, m_i, at each floor (i). Recognizing that the first mode shape may vary with β_{CB}, thus

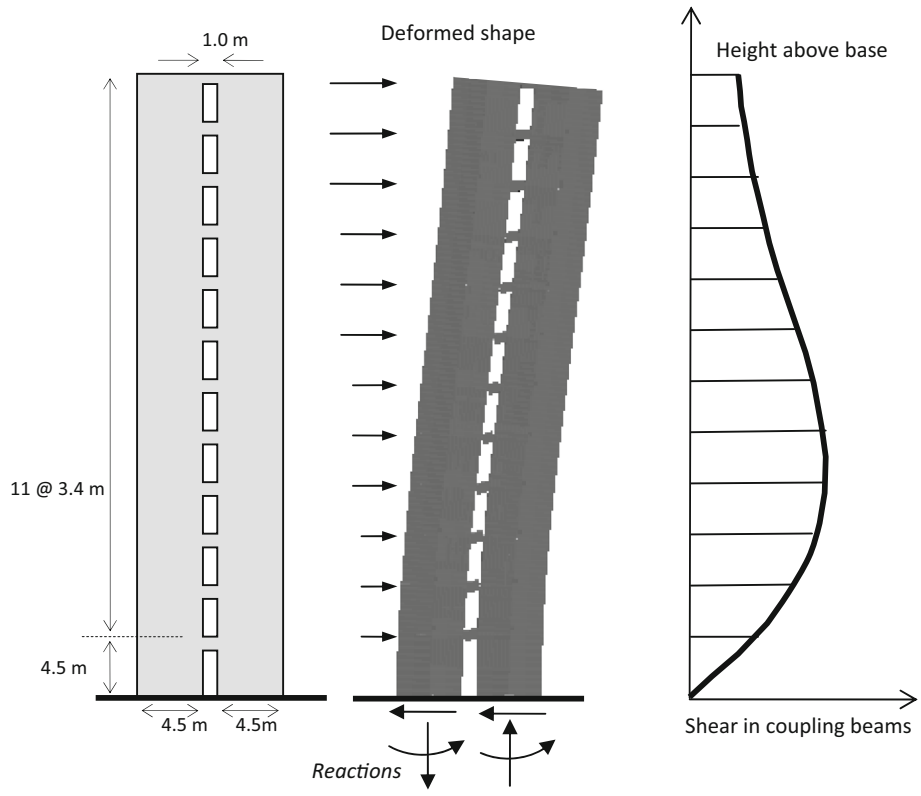

Fig. 2 Deformed shape (exaggerated) and coupling beam shear distribution during the linear elastic response of a 12-story coupled wall.

affecting the lateral force distribution and moments (and curvatures) over the heights of the walls, analytical studies were conducted to calibrate a simple expression for the yield displacement of a cantilever wall.

Consider first that a cantilever wall, loaded by a single force at the roof, has a linear distribution of bending moment that reaches a peak at its base. Assuming that all sections have the same stiffness, the curvature distribution varies linearly from the roof to the base. When the maximum curvature (at the base of the wall) is the yield curvature, $\emptyset_y$, the displacement at the top of the wall is given (by integrating the curvature twice) as:

$$D_y = \phi_y \frac{H^2}{3} \tag{2}$$

where H is the height of the wall.

Now, consider that based on common approximations of the yield curvature for other structural elements (Table 1 and Hernández-Montes and Aschheim 2003; Priestley et al. 2007), the yield curvature ($\emptyset_y$) may be represented parametrically as

$$\phi_y = \kappa \frac{\varepsilon_y}{D_{cw}} \tag{3}$$

where ε_y is the yield strain of the reinforcing steel and κ is a coefficient to be deduced for coupled walls that accounts for the complicated mechanical behavior of coupled walls undergoing response in a first-mode pushover analysis. The depth of the wall, D_{cw}, in Eq. 3 is the distance between the center of gravity of the primary longitudinal reinforcement at one boundary of the coupled wall and the extreme concrete fiber of the remote edge (i.e., the overall section height of the cross section of the entire coupled wall less the cover to the centroid of the boundary longitudinal reinforcement), as illustrated in Fig. 3.

3. Numerical Study of Coupled Walls

To calibrate the value of κ in Eq. 3, and to evaluate the applicability of this approach for a relevant range of coupled walls, three sets of coupled walls were studied, having 8, 12, and 20 stories above the base. The cross section and

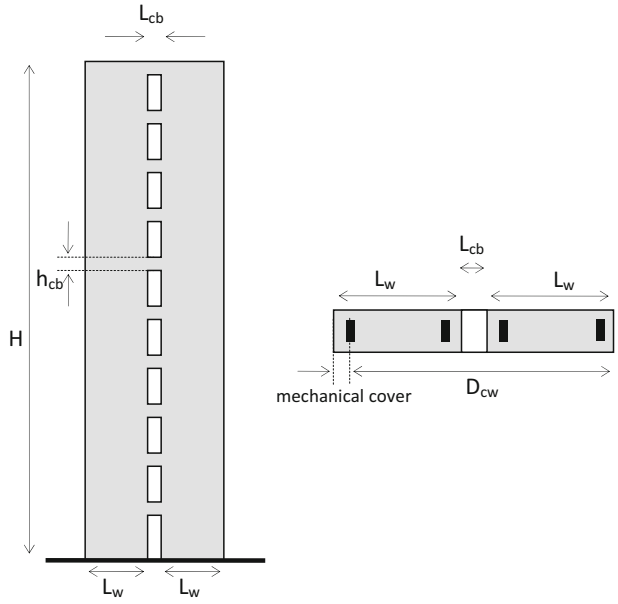

Fig. 3 Nomenclature.

coupling beam dimensions are shown in Fig. 4, which illustrates the 12-story coupled wall. A plan view applicable to the three sets is also shown, which shows the floor plan that is common to all stories. Ordinary steel and concrete materials are used—using Eurocode designations, the reinforcing steel is B500 (having characteristic strength $f_{yk} = 500$ MPa and expected yield strength of 575 MPa) and the concrete is C-30 (having characteristic strength $f_{ck} = 30$ MPa and expected compressive strength of 39 MPa) for all the walls.

The design of coupling beams is normally governed by shear strength limits. Thus, the analytical study considered two design shear levels, 500 and 1000 kN, representing unit shear stresses on the gross section of 0.33 and 0.65 $\sqrt{f_{ck}}$ (MPa units) and 3.95 and 7.91 $\sqrt{f'_c}$ (psi units), and corresponding bending moment strengths at the wall face of 250 and 500 kN m (184 and 369 k-ft), respectively, following EC-2 (2002).

Figure 5 illustrates the reinforcement of each wall pier with 22Ø25 (corresponding to $0.006A_c$, between the limits of $0.002A_c$ and $0.04A_c$). An additional case was considered, in which the longitudinal reinforcement within the end zone is increased by 50%. Thus, two levels of longitudinal

Table 1 Estimates of yield curvature provided in Priestley et al. (2007).

Circular concrete column	$2.25\varepsilon_y/D$
Rectangular concrete column	$2.10\varepsilon_y/h_c$
Rectangular concrete wall	$2.00\varepsilon_y/l_w$
Symmetrical steel section	$2.10\varepsilon_y/h_s$
Flanged concrete beam	$1.70\varepsilon_y/h_b$

where ε_y is the yield strain of the reinforcing steel, and D, h_c, l_w, h_s and h_b are the depths of the circular column, rectangular column, rectangular wall, steel section and flanged concrete beam sections, respectively. One may notice a distinction in that expressions of the yield curvature initially were functions of the overall height of the member section (Priestley et al. 1995), while later studies (Hernández-Montes and Aschheim 2003) introduced the effective depth (to the centroid of the tension reinforcement) as a more physically meaningful term in yield curvature expressions for RC members.

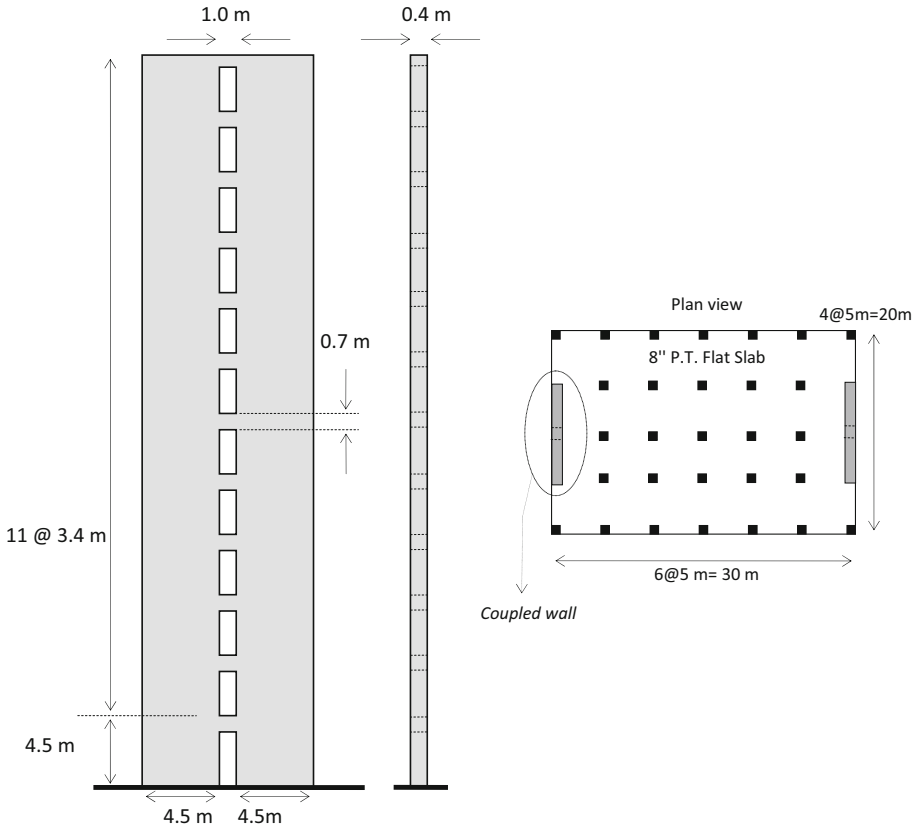

Fig. 4 Elevation of 12-story building, and floor plan applicable to 8, 12, and 20-story buildings.

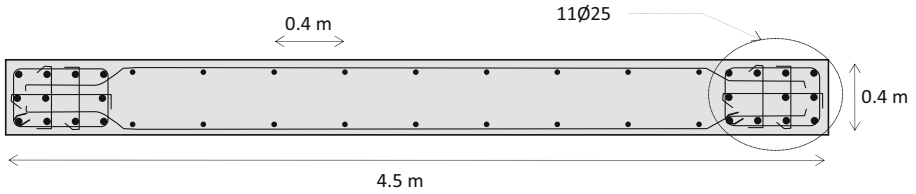

Fig. 5 Cross-section of one wall pier.

reinforcement at the base of the wall were considered, for the 8-, 12-, and 20-story buildings.

In the uniform coupled wall cases considered herein, where cross sectional dimensions of all components and reinforcement within the coupling beams is held uniform, the proportion of overturning moment resisted at the base of the wall system resisted by the coupling action (represented by β_{CB}) increases as the number of stories increase. As will be shown later in the paper, yielding at the base of the wall may be postponed to much later in the lateral (pushover) analysis. As the number of stories increases, the reinforcement provided at the base of the wall has less influence on the lateral strength of the coupled wall because the resistance provided by the coupled beams may be substantial.

The walls were modeled using fiber elements, with steel and concrete materials represented at their expected strengths of $f_{ye} = 575$ MPa and $f_{ce} = 39$ MPa rather than at the nominal characteristic strengths. The models of each coupled wall were subjected to nonlinear static (pushover) analysis using lateral forces applied to the coupled wall in proportional to the first mode forces. The applied force to story i is F_i, defined by EC-8 (§ 4.3.3.2.3) (2004).

$$F_i = F_b \frac{s_i m_i}{\sum s_j m_j} \tag{4}$$

where F_b is the shear at the base of the wall, and s_i and s_j are the displacements of masses m_i, m_j, respectively, in the fundamental mode. The pushover curve is obtained using a displacement-controlled analysis, in which the roof displacement is gradually increased with F_b adjusted to provide equilibrium at the nodes. The results are typically displayed as a "capacity curve," which plots F_b on the ordinate and roof displacement on the abscissa.

Figure 6 shows the capacity curves determined for the four coupled walls of the 8-story set. The solid lines

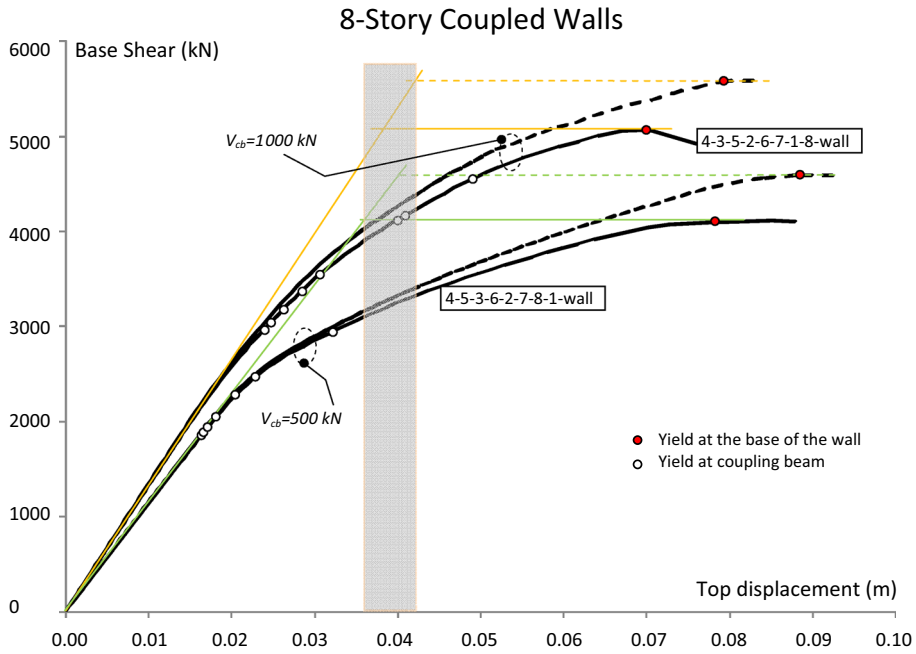

Fig. 6 Capacity curves for the set of 8-story coupled walls.

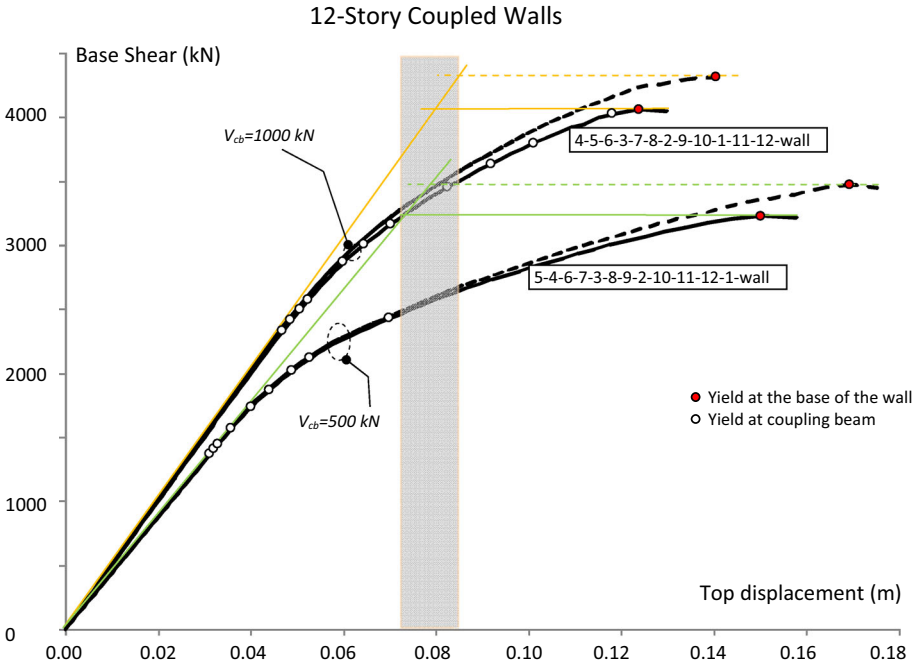

Fig. 7 Capacity curves for the set of 12-story coupled walls.

correspond to the reinforcement of the wall shown in Fig. 5, and the dashed lines represent the response of walls having 50% greater area of longitudinal reinforcement. The lower two curves correspond to a coupling beam shear resistance of V = 500 kN, while the upper two curves correspond to a coupling beam shear resistance of V = 1000 kN. The series of numbers in the boxes identify the sequence of yielding of the coupling beams. The yield displacement is defined as the intersection of the horizontal line that marks the maximum value of the base shear and the inclined line defined by the slope in the linear range, representing cracked section behavior (Fig. 6). It can be seen that the yield displacement stays in a narrow segment whose mean value is 0.039 m for the 8-story coupled walls (or 0.14% of the height of 28.3 m).

Similarly, Figs. 7 and 8 show that the mean yield displacement for the 12-story coupled walls and for the 20-story coupled walls is 0.0785 and 0.198 m, respectively. This corresponds to 0.19% of the height of the 12-story coupled walls (41.9 m) and 0.29% of the height of the 20-story coupled walls (69.1 m).

It can be observed that solid lines and dashed lines get closer as the number of stories of the coupled walls increases, as shown in Figs. 6, 7, and 8. For the case of 20-story wall and V_{cb} = 500 kN, both lines coincide. This is

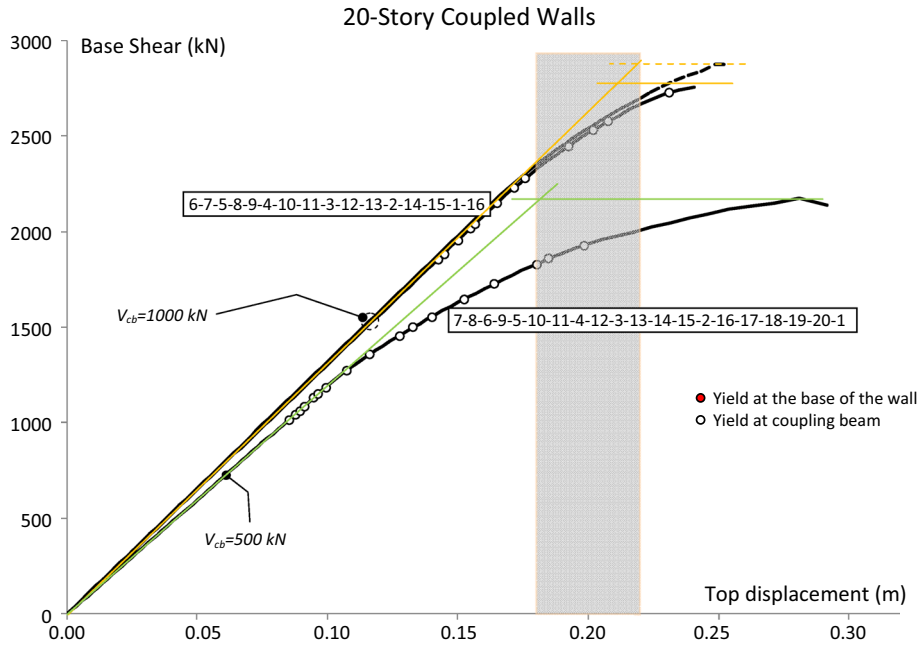

Fig. 8 Capacity curves for the set of 20-story coupled walls.

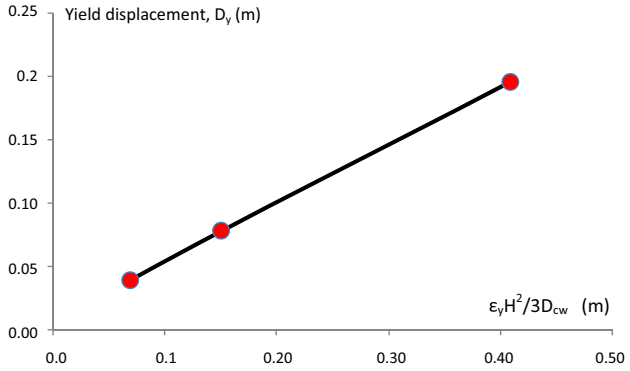

Fig. 9 Mean yield displacements of the three sets of coupled walls.

congruent with the fact already commented that as the number of stories increases, the reinforcement provided at the base of the wall has less influence on the lateral strength of the coupled wall.

Introducing Eq. 3 into Eq. 2:

$$D_y = \kappa \frac{\varepsilon_y}{D_{cw}} \frac{H^2}{3} \tag{5}$$

Figure 9 plots mean values of D_y as a function of $\varepsilon_y H^2/3D_{cw}$ for the three sets of coupled walls. The empirical results are approximately linear; the slope of the curve provides an estimate of κ equal to 0.52 for the coupled walls. Therefore, an estimate of the displacement at the top of a coupled wall at yield in a first mode pushover analysis is given by:

$$D_y = 0.52 \frac{\varepsilon_y}{D_{cw}} \frac{H^2}{3} \tag{6}$$

where "yield" is defined as the intersection of the bilinear curves that were fitted to the analytical results of Figs. 6, 7, and 8.

4. Example of Seismic Design Based on an Estimated Yield Displacement

In this section the preliminary design of a coupled wall is developed to illustrate how the estimated yield displacement can be used in seismic design. First, the design is based on application of the equal displacement rule to an elastic design spectrum. Then, to illustrate an alternative approach, Yield Point Spectra are used.

The coupled wall is part of the perimeter of a 12-story RC frame structure (Fig. 4). The height of the first story is 4.5 m while the overlying stories are 3.4 m high, resulting in a total height of 41.9 m. The coupled wall consists of two rectangular section walls having a plan length of 4.5 m and thickness of 0.4 m. B500 steel reinforcement (f_{yk} = 500 MPa) and C-30 concrete (f_{ck} = 30 MPa) are used. The material safety factors used in the design are $\gamma_s = 1.0$ and $\gamma_c = 1.0$.

The seismic design performance objectives are: first to limit the interstory drift ($D_{u,drift}$) given by EC-8 (§4.4.3.2) to

$$D_{u,drift}\nu = 0.0075\ h \tag{7}$$

where $\nu = 0.5$ for buildings of importance classes I and II, and second to limit the ductility demand to the value given by the EC-8 behavior factor ($q = 3.6$) for coupled walls of medium ductility (§5.2.2.2).

The seismic action is calculated based on EC-8 (2004). The horizontal seismic action is represented by the elastic response spectrum Type 1 (Ms >5.5, EC-8 §3.2.2.2 where

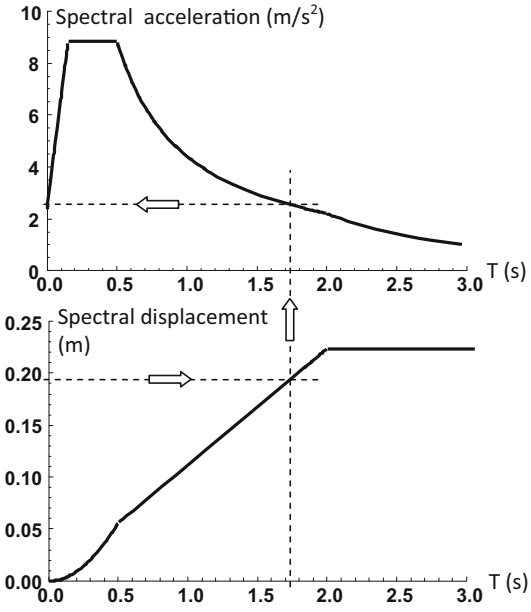

Fig. 10 Elastic spectra of pseudo-accelerations and displacements.

Ms is the surface-wave magnitude). The type of soil is B (EC-8 Table 3.1), and according EC-8 Table 3.2: $T_B = 0.15$ s, $T_C = 0.5$ s, $T_D = 2.0$ s, and $S = 1.2$. T_B and T_C are the lower and the upper limit of the period of the constant spectral acceleration branch, respectively. T_D is the value defining the beginning of the constant displacement response range of the spectrum and S is the soil factor.

The reference peak ground acceleration is $a_{gR} = 0.3$ g, where g is the acceleration of the gravity. The building is classified as importance class II, meaning $\gamma_I = 1.0$ [EC-8 Table 4.3 and §4.2.5(5), where γ_I is the importance factor]. Thus the peak ground acceleration $a_g = \gamma_I a_{gR} = 0.3$ g. Damping of 5% is considered by imposing $\eta = 1.0$.

4.1 Design Based on an Elastic Spectrum

The elastic pseudo-acceleration response spectrum (q = 1) given in EC-8 §3.2.2.5 and corresponding displacement spectrum [$S_{d,displ} = S_d(T/2\pi)^2$] are shown in Fig. 10.

Application of the drift limit corresponds to a peak roof displacement of

$$D_{u,\,drift} = 0.0075\frac{h}{v} = 0.0075\frac{41.9}{0.5} = 0.62 \text{ m} \tag{8}$$

The roof displacement at yield is estimated using Eq. 6,

$$D_y = 0.52\frac{\varepsilon_y}{D_{cw}}\frac{H^2}{3} = 0.52\frac{500/200,000}{9.75}\frac{41.9^2}{3} = 0.078 \text{ m} \tag{9}$$

Thus, application of the ductility limit of q = 3.6 for a wall of medium ductility class results in a roof displacement limit of

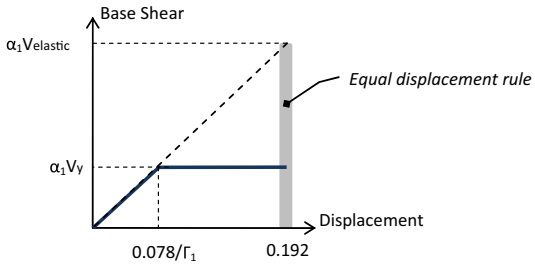

Fig. 11 Equal displacement rule.

$$D_{u,\,ductility} = \mu D_y \approx qD_y = 3.6 \cdot 0.078 \text{ m} = 0.281 \text{ m} \tag{10}$$

Since we wish to exceed neither the drift nor the ductility limits, the more restrictive roof displacement limit of 0.281 m applies. Noting that the first mode participation factor, Γ_1, should be approximately 1.46 for a coupled wall building 12 stories in height (NEHRP 2009), the associated peak displacement of an "equivalent" SDOF system (NEHRP 2009) is

$$D_u^* = \frac{D_u}{\Gamma_1} = \frac{0.281}{1.46} = 0.192 \text{ m} \tag{11}$$

Since we expect the equal displacement rule (Fig. 11) to apply to structures with periods greater than T_C, we can use the spectral displacement plot of Fig. 10 to determine the period of a long-period system whose spectral displacement is 0.192 m. This period is 1.72 s; the corresponding pseudo-spectral acceleration (S_d) value (Fig. 10) is 2.57 m/s^2.

Considering similar triangles, the required S_d value for the yielding SDOF oscillator is given by (2.57 m/s^2)(0.078/1.46/0.192) = 0.72 m/s^2.

The tributary mass per story is 234,000 kg; the total reactive weight is (234,000 kg)(12)(9.81 m/s^2)(1 kN/1000 N) = 27,546 kN. The first-mode effective mass coefficient α_1 is approximately 0.79 for a coupled wall building of this height (NEHRP 2009). Therefore, the required base shear strength at yield is estimated to be 0.79(0.72 m/s^2)(27,546 kN)/(9.81 m/s^2) = 1597 kN.

4.2 Design Using Yield Point Spectra

Yield Point Spectra were generated considering the elastic response spectrum reduced by assumed values of the behavior factor q, representing different ductilities (EC-8, §3.2.2.5). The design spectrum is plotted with ordinate S_d and abscissa yield displacement D_y, determined parametrically as a function of T. The spectral design acceleration $S_d(T)$ is given by EC-8 (§3.2.2.5), while $D_y(T)$ is given by:

$$D_y(T) = \frac{F_y}{k} = \frac{S_d(T)\ m}{\omega^2\ m} = S_d(T)\left(\frac{T}{2\pi}\right)^2 \tag{12}$$

Figure 12 shows the EC-8 Design Spectra in a Yield Point Spectra representation, for q = 1, 3.6 and 8.0.

The following flowchart shows the steps taken to obtain the initial design of the structure (Fig. 13).

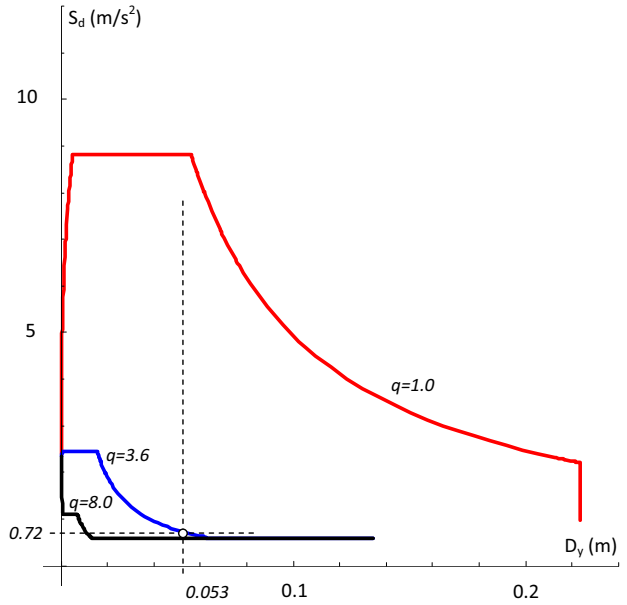

Fig. 12 Yield Point Spectra representation of EC-8 Design Spectra.

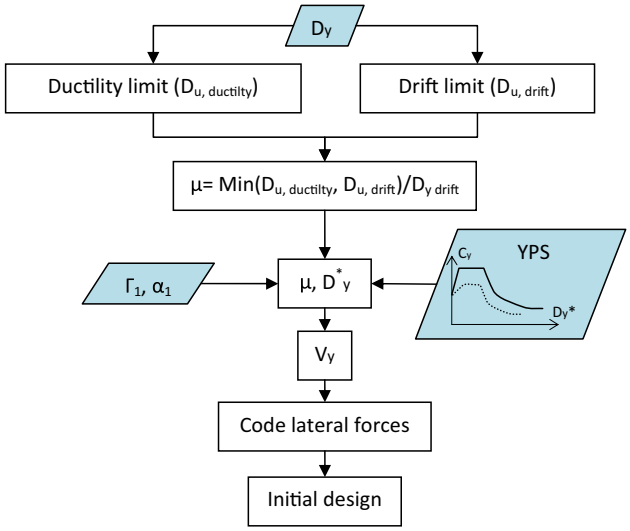

Fig. 13 Design method.

As before, the roof displacement at yield is estimated according to Eq. 6 as

$$D_y = 0.52\frac{\varepsilon_y}{D_{cw}}\frac{H^2}{3} = 0.52\frac{500/200,000}{9.75}\frac{41.9^2}{3} = 0.078 \text{ m} \tag{13}$$

Application of the drift limit is associated with a peak roof displacement of

$$D_{u,\,drift} = 0.0075\frac{h}{v} = 0.0075\frac{41.9}{0.5} = 0.62 \text{ m} \tag{14}$$

Because we have estimated D_y be 0.078, the q factor for this limit is $q \approx \mu = D_{u,drift}/D_y = 7.95$.

Similarly, the roof displacement associated with the ductility limit of q = 3.6 is determined as

$$D_{u,\,ductility} = \mu D_y \approx qD_y = 3.6 \cdot 0.078 \text{ m} = 0.281 \text{ m} \tag{15}$$

The corresponding design spectra for both values of q in a yield point representation are shown in Fig. 12. As in previous section, we use an estimate of the first modal participation factor of $\Gamma_1 = 1.46$. Therefore, we enter the Yield Point Spectra with an estimated yield displacement of

$$D_y^* = \frac{D_y}{\Gamma_1} = \frac{0.078}{1.46} = 0.053 \text{ m} \tag{16}$$

The required yield strength coefficient to meet both performance objectives is associated with the smaller value of q. Therefore, in this case, the system design is controlled by ductility limits and not by interstory drift limits. The ductility limit for design is 3.6. According to Fig. 12 the required spectral acceleration is $S_d = 0.72$ m/s^2. The associated period of vibration, applicable to both the SDOF system and the first mode of the MDOF system, is

$$T = 2\pi\sqrt{\frac{D_y^*}{S_d}} = 1.72 \text{ s} \tag{17}$$

The result is identical to that obtained in Sect. 4.1. However, the Yield Point Spectra format may be appreciated as more direct, and applies more generally, including portions of the spectrum where short period displacement amplification is present.

As previously calculated, the required base shear strength at yield is $V_b = 1597$ kN. The horizontal seismic forces can then be calculated according to EC-8 §4.3.3.2.3(3).

Table 2 Horizontal forces.

Story	F_i (kN)
12	240
11	221
10	201
9	182
8	162
7	143
6	123
5	104
4	84
3	65
2	45
1	26
0	0

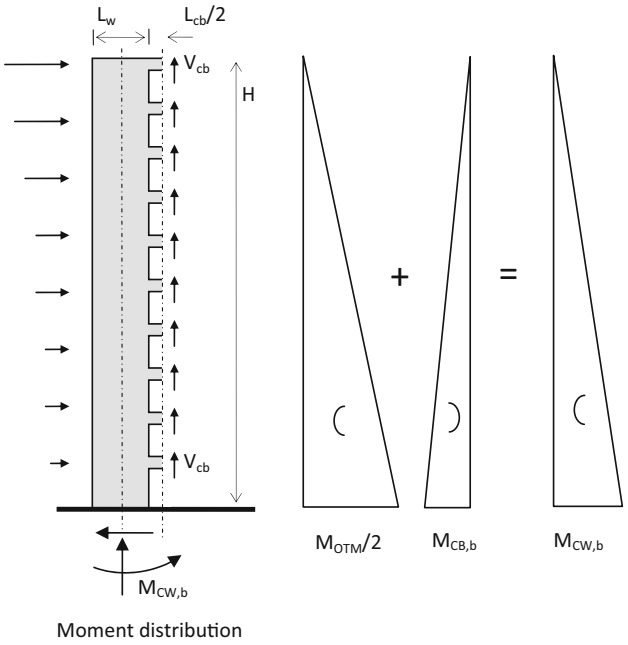

Fig. 14 Mechanism analysis.

The overturning moment, M_{OTM}, at the base of the coupled wall, due to the horizontal seismic forces indicated in Table 2 is

$$M_{OTM} = \sum_i F_i h_i = 46,539 \text{ kN m} \tag{18}$$

In order to calculate the reinforcement in the members, the value of β_{CB} (Priestley et al. 2007) is chosen. β_{CB} should be established for design between 0.25 and 0.75 (Priestley et al. 2007). In this example, we chose β_{CB} to be equal to 0.4.

$$\beta_{CB} = \frac{M_{CB,b}}{M_{OTM}} = 0.4 \;\Rightarrow\; M_{CB,b} = 0.4 M_{OTM} \tag{19}$$

where $M_{CB,b}$ is the total moment of the coupling beams at the base. Assuming that the shear carried by all coupling beams is identical (V_i), with the coupling beams having dimensions $L_w = 4.5$ m and $L_{CB} = 1.0$ m, then V_i is equal to 564.1 kN

$$\begin{aligned} M_{CB,b} &= \sum_{i=1}^{12} V_i (L_w/2 + L_{cb}/2) \;\rightarrow \\ V_i &= \frac{0.4 \cdot 46,539}{12(4.5/2 + 1/2)} = 564.1 \text{ kN} \end{aligned} \tag{20}$$

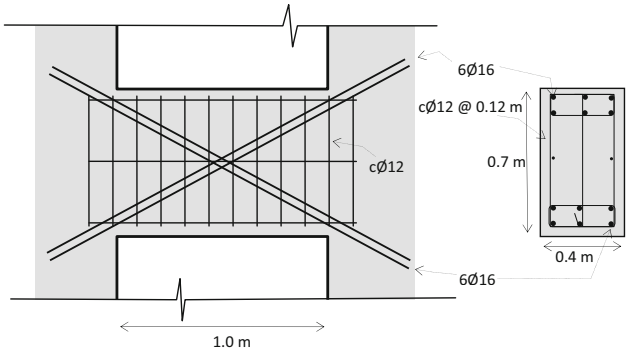

Fig. 16 Reinforcement of the coupling beams.

At the same time, assuming that the ultimate behavior of the wall is described by the mechanism shown in Fig. 14, the required flexural strength of each of the two walls at the base, $M_{CW,b}$, is

$$M_{CW,b} = \frac{M_{OTM}}{2} - M_{CB,b} = 4654.2 \text{ kN m} \tag{21}$$

The moment at the base, $M_{CW,b}$, acts with an axial force in tension of 3150 kN. The cross section of Fig. 15, designed following EC-2 prescriptions, contains 10ϕ25 bars within each boundary.

Each coupling beam is designed to resist a shear $V_i = 564.1$ kN, along with a flexural moment of 282.1 kN m at the face of the wall. The resulting reinforcement is indicated in Fig. 16.

The coupled wall was modeled using SeismoStruct (2016), with concrete modeled assuming $f_{ce} = 1.3 \cdot f_{ck} = 39$ MPa (per Priestley et al. 2007) and steel modeled assuming $f_{ye} = 1.15 \cdot f_{yk} = 575$ MPa. The resulting period is 1.7 s. Because this period is slightly less than 1.72 s, we are confident the spectral displacement will be acceptable. An eigenvalue analysis of the preliminary design determined $\Gamma_1 = 1.47$, which is very close to the value of 1.46 assumed at the start of the design process. The eigenvalue analysis determined $\alpha_1 = 0.62$, which is less than the value of 0.79 assumed when establishing the design base shear. Relative to the values assumed in preliminary design, the reduction in period will cause the spectral displacement to be slightly smaller, while the increase in Γ_1 will cause a slight increase in the roof displacement relative to the spectral displacement, representing a minor combined effect. Design for the higher value of α_1 confers greater lateral strength than is needed (which is also reflected in greater stiffness that results in a slightly lower period). While the

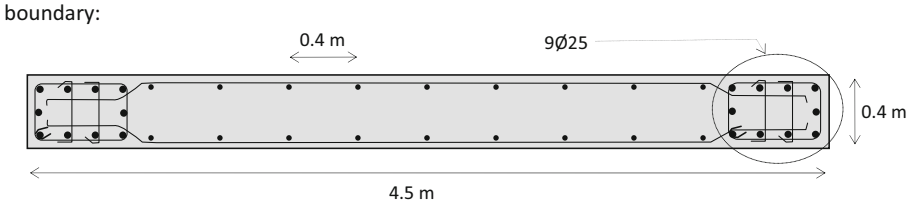

Fig. 15 Longitudinal reinforcement of the wall.

ductility and interstory drift demands should be acceptable, a minor refinement using the values of Γ_1 and α_1 determined for the initial design can be done, if such precision is needed.

In comparison, the EC-8 estimate of period for a coupled wall of this height is given by $0.05H^{3/4} = 0.823$ s. Similarly, the ASCE-7 (§12.8.2.1) estimate is 0.804 s. These two estimates of period, relied upon in conventional code-based seismic design approaches, are suggested without regard to lateral strength, stiffness, or mass, and thus are seen to be less precise than that determined based on seismic performance objectives and an estimate of the yield displacement. Because the code period estimates are less than half of the computed first mode period, peak displacements would be substantially underestimated using the code period estimates; any updating to recognize the eigenvalues would necessitate a series of iterative design refinements. The approaches herein (Sects. 4.1 and 4.2) led to an excellent preliminary design in a single step. Past behaviors of walls under earthquake motions (Wallace 2012; Kim et al. 2016) force us to consider improvements in the design.

In the case of walls with non-uniform coupling beams, walls having different geometry, or non-uniform mass distributions or story heights, the yield displacement will deviate from the estimates developed herein. However, the stability of the yield displacement will apply to these systems as well, i.e., the yield displacement observed in a first mode pushover analysis will remain approximately constant for proportional changes in strength. Thus, the estimate of yield displacement and modal parameters used in the initial design can be updated using values computed in the analysis of the first design.

5. Conclusions

New expressions to estimate the yield displacement of coupled wall systems in a nonlinear static (pushover) analysis are presented herein. The expressions were calibrated to uniform coupled walls having a range 8–20 stories, for wall cross-sections of 10×0.4 m, with coupling beams of $1 \times 0.7 \times 0.4$ m and story heights of 3.4 m. The expressions are stated in terms of parameters that are known or may be estimated early in the design process. A design example using an "equivalent" single-degree-of freedom system in conjunction with Yield Point Spectra was provided to illustrate the application of these estimates to the design of a RC coupled wall. The design example and method more generally demonstrates that the fundamental period of vibration is a consequence of the lateral strength (and stiffness) provided to satisfy the seismic performance objectives, and is estimated with poor fidelity by current code formulae for the so-termed "approximate period," T_a. The accuracy of the yield displacement estimate allowed the preliminary design to be achieved in a single step, whereas the use of conventional code estimates of fundamental period of vibration is likely to require a series of design iterations in order to obtain a preliminary design that achieves the desired seismic performance objectives.

Open Access

References

Aschheim, M. A. (2000). The primacy of the yield displacement in seismic design. In *Second US–Japan workshop on performance based design of reinforced concrete buildings*, Sapporo, Japan, September 10–12, 2000.

Aschheim, M. A., & Black, E. F. (2000). Yield Point Spectra for seismic design and rehabilitation. *Earthquake Spectra, EERI, 16*(2), 317–335.

Eurocode 2 (2002, July). *Design of concrete structures—Part 1*: *General rules and rules for buildings.* prEN 1992-1-1. Brussels: European Committee for Standardization.

Eurocode 8 (2004, April). *Design of structures for earthquake resistance—Part 1*: *General rules*, *seismic actions and rules for buildings*. EN1998-1. Brussels: European Committee for Standardization.

Hernández-Montes, E., & Aschheim, M. (2003). Estimates of the yield curvature for design of reinforced concrete columns. *Magazine of Concrete Research, 55*(4), 373–383.

Kim, J., Jun, Y., & Kang, H. (2016). Seismic behavior factors of RC staggered wall buildings. *International Journal of Concrete Structures and Materials, 10*(3), 355–371.

Naeim, F. (2001). *The seismic design handbook* (2nd ed.). Boston: Kluwer Academic Publishers.

NEHRP recommended seismic provisions for new buildings and other structures, 2009 edition. Resource Paper 9: Seismic design using target drift, ductility, and plastic mechanisms as performance criteria.

Paulay, T. (2002a). A displacement-focused seismic design of mixed building systems. *Earthquake Spectra, 18*(4), 689–718.

Paulay, T. (2002b). An estimation of displacement limits for ductile systems. *Earthquake Engineering and Structural Dynamics, 31,* 583–599.

Priestley, M. J. N., Calvi, G. M., & Kowalsky, M. J. (2007). *Displacement-based seismic design of structures*. Pavia: IUSS Press.

Priestley, M. J. N., Seible, F., & Calvi, M. (1995). *Seismic design and retrofit of bridges*. New York: Wiley.

SeismoStruct (2016). www.seismosoft.com.

Tjhin, T. N., Aschheim, M. A., & Wallace, J. W. (2007). Yield displacement-based seismic design of RC wall buildings. *Engineering Structures, 29*(11), 2946–2959.

Wallace, J. W. (2012). Behavior, design, and modeling of structural walls and coupling beams—Lessons from recent laboratory tests and earthquakes. *International Journal of Concrete Structures and Materials, 6*(1), 3–18.